Journal of Solid Mechanics Vol. 10, No. 2 (2018) pp. 338-353

Fatigue Life of Graphite Powder Mixing Electrical Discharge Machining AISI D2 Tool Steel

A. Al-Khazraji [1], S.A. Amin [1], S.M. Ali [2,*]

[1]*Mechanical Engineering Department, University of Technology, Baghdad, Iraq*
[2]*Biomedical Engineering Department, University of Technology, Baghdad, Iraq*

Received 3 March 2018; accepted 27 April 2018

ABSTRACT

The present paper deals with the design of experimental work matrices for two groups of experiments by using Response surface methodology (RSM). The first EDM group was dealt with the use of kerosene dielectric alone, while the second was treated by adding the graphite micro powders mixing to dielectric fluid (PMEDM). The total heat flux generated and fatigue lives after EDM and PMEDM models were developed by FEM using ANSYS 15.0 software. The graphite electrodes gave a total heat flux higher than copper electrodes by (82.4 %). The use of graphite powder and both electrodes yielded more heat flux by (270.1 %) and (102.9 %) than the copper and graphite electrodes, respectively with use of kerosene dielectric alone. Using graphite electrodes and kerosene dielectric alone improved the WLT by (40.0 %) when compared with the use of copper electrodes. Whereas, using copper electrodes and the graphite powder improved the WLT by (66.7 %) compared with the use of graphite electrodes under the same machining conditions. Copper electrodes with graphite powder gave experimental fatigue safety factor higher by (30.38 %) when compared with using graphite electrodes and higher by (15.73%) and (19.77%) when compared with using the copper and graphite electrodes and kerosene dielectric alone, respectively.

© 2018 IAU, Arak Branch. All rights reserved.

Keywords: EDM; PMEDM; Graphite powder; RSM; ANOVA; FEM; AISI D2 Die Steel; WLT; Total heat flux; Fatigue life; Fatigue safety factors.

1 INTRODUCTION

THE characteristics and the white layer thickness (WLT) are closely related to the phase transformation which takes place during the solidification process. This in turn is dependent on the chemical composition of the original work piece, the heat treatment conditions applied prior to machining, and the EDM machining parameters most notably the pulse current and the pulse-on duration. The depth and size of the cracks formed on the recast layer increase as the heat energy per spark increases [1-2]. It consists of micro-cracks and high tensile residual stresses on the EDMed surface caused by the high temperature gradient [3]. The adverse effect of discharge energy also provided some insights on the fatigue strength of the work piece, which propagates from the multiple surface imperfections within the recast layer [4]. The mixing powder into the dielectric fluid is called powder mixed EDM

*Corresponding author. Tel.: +96 47803700877.
E-mail address: saad.eng@uokerbala.edu.iq (S.M.Ali).

© 2018 IAU, Arak Branch. All rights reserved.

(PMEDM) which reduces its insulating strength and increases the spark gap distance between the tool and work piece to spread the electric discharge uniformly in all directions. As a result; the process becomes more stable, thereby improving the material removal rate (MRR) and surface finish [5-6]. Many researchers have proposed improving the fatigue life of EDM component by using a post-machining operation to remove the recast layer or to coat the machined surface with a metallic layer. However, both methods inevitably extend the manufacturing time and increase the manufacturing cost. The current study conducts an experimental investigation of two methods (the powder mixing that does not need post-treatment processing, and the economic and quick shot blast peening process) to identify the optimal EDM machining parameters which suppress the formation of cracks in the recast layer for longest lives under different fatigue loads.

The objective of this study deals with the developing numerical models and verifying the experimental results by using the response surface methodology (RSM) and the finite element method (FEM) with ANSYS 15.0 software for study the effects of graphite powder mixing (PMEDM) parameters on the total heat flux generated, white layer thickness (WLT) and fatigue life properties of the selected AISI die steel workpiece.

2 EXPERIMENTAL WORK

Two types of electrodes materials were selected (Copper and Graphite) with dimensions of $30 \times 24 \times 24$ *mm*. The copper electrode material was examined for chemical composition properties using the X-Met 3000TX Horizontal metal analyzer. The average grain size for graphite powder is (44,866 μm).

The EDM parameters are; the gap voltage V_P (140V), the pulse on time duration period T_{on} (40 and 120 μs), the pulse off time duration period T_{off} (14 and 40 μs), the pulse current I_P (8 and 22 A), the duty factor (η = 75%), two sides flashing pressure = 0.73 bar (10.3 *psi*.) and the graphite powder mixing concentration = (0 and 5*gm/lit*). The work piece material was prepared for chemical composition, mechanical properties tests and Rockwell hardness tests on the bases of ASTM-77 steel standard for mechanical testing of steel products [7]. The work piece specimens were prepared with dimensions $89.9 \times 30 \times 4.25$ *mm*, according to requirement of the Avery type 7305 plain bending fatigue testing machine shown in Fig. 1.

The average values of chemical composition of the selected work piece material and the equivalent values given according to ASTM A 681-76 standard specification for alloy and die steels [8] are listed in Table 1. The results of tensile test and Rockwell hardness tests are given in Table 2. The chemical composition of the copper electrodes is listed in Table 3. The used kerosene dielectric was tested according to the ASTM (D 3699-90) industry standard specifications for kerosene. The chemical composition of the graphite powder was tested for compositions by using the *X*-Ray diffraction tester. A stainless steel container was fabricated for the purpose of powder mixing with the dielectric fluid (PMEDM). The CNC ACRA type EDM machine with all the fabricated accessories is shown in Fig. 2. In this work, two groups were planned, each containing (22) experiments using a new set of work piece and electrode in each experiment. The first (11) experiments in each group were machined by using the copper electrodes, while the last (11) experiments were done by using the graphite electrodes. The work pieces after EDM machining with the used copper and graphite electrodes for both groups are shown in Fig. 3.

Table 1
The chemical compositions of workpiece material.

SAMPLE	C %	Si %	Mn%	P %	S %	Cr %	Mo %	Ni %	Co %	Cu %	V %	Fe %
Tested (Average)	1.51	0.174	0.264	0.014	0.003	12.71	0.555	0.158	0.0137	0.099	0.306	Bal.
Standard AISI D2	1.40 to 1.60	0.60 max.	0.60 max.	0.03 max.	0.03 max.	11.00 to 3.00	0.70 to 1.20	-	1.00 Max.	-	1.10 Max.	Bal.

Table 2
The mechanical properties of the selected materials.

Sample	Ultimate tensile stress *N/mm²*	Yield strength *N/mm²*	Elongation %	Hardness HRB
Average	704.25	415.25	18.125	90.75

Table 3
The chemical compositions of copper electrodes material.

Zn%	Pb%	Si%	Mn%	P%	S%	Sn%	Al%	Ni%	Sb%	Fe%	Cu%
0.006	0.001	0.011	0.0002	0.005	0.002	0.0005	0.007	0.004	0.005	0.007	99.96

© 2018 IAU, Arak Branch

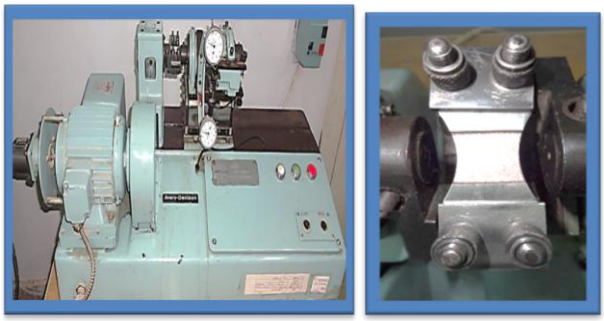

Fig.1
The Avery Denison plain bending fatigue testing machine type 7305, England.

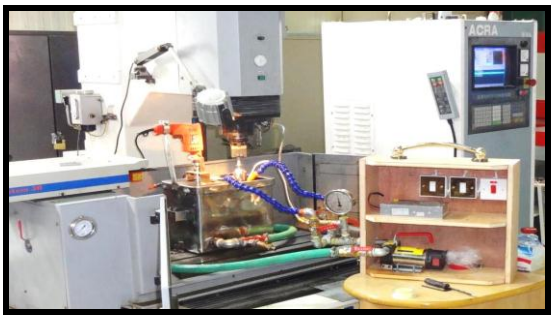

Fig.2
The (CNC) EDM machine with all the fabricated accessories.

1 2

Fig.3
The specimens and the used copper and graphite electrodes for groups (1 and 2) experiments after EDM and PMEDM machining.

3 MODELING AND SIMULATION THE HEAT FLUX USING FEM

The Gaussian distribution of heat applied at the axis of a spark for a single discharge has a maximum radius (R), and then the heat flux (Qw) at radius (r) of the system is given by the following relation [9]:

$$Qw\,(r) = \frac{4.57 * Rw\ * Vb * Ip * Kn}{\pi . R^{2}} e^{-4.5\frac{r^{2}}{R^{2}}} \tag{1}$$

The rate of energy incident on the work piece is equal to the rate of energy supplied which is equal to $Rw*V_P*I_P$. Where, Rw is the energy percentage fraction of heat input to the work piece, Vb is the breakdown voltage (different from the applied voltage), R is the spark radius in μm, and I_P is the discharge current. The breakdown voltage value (Vb) was taken as (20 V), while for PMEDM it was about 20% – 30% lower than that for EDM, i.e., Vb =15 V. The spark radius (R) was taken as (15 μm), and the heat flux for AISI D2 die steel is ($Qw\,(r)$ = 680 MW/m^2K) for various values of discharge current. The spark radii for PMEDM processes was taken to be 40% larger than traditional EDM.

© 2018 IAU, Arak Branch

The (*Rw*) is the value that has been determined by Yadav et al. [10] and Patel et al. [11] who have suggested that a constant fraction of total power is transferred to the electrodes. They have used the value of (*Rw*) as 8% as the percentage of heat input absorbed by the work piece for their theoretical work of conventional EDM and the same value was used in this work. The *Rw* values during PMEDM in the present model have been assumed to be 9% of the total heat lost in the work piece. Shankar et al. [12] have calculated that about 18% is absorbed by cathode and the rest is discharged to the dielectric fluid.

The new parameter (*Kn*) which takes into account the effect of suspended powder particles on the spark frequency and breakdown voltage was also calculated. The value of (*Kn*) depends upon the type of powder, the powder properties, such as shape, size, concentration, etc. The values of (*Kn*) factor were experimentally estimated for EDM and PMEDM machining groups as given in Table 4. using the results of material removal rates which were experimentally determined. Marafona et al. [13] suggested an equation called the equivalent heat input radius *R(t)* or the radius of plasma channel (μm), which is dependent on the current intensity (I_P) and pulse on duration (T_{on}), there by:

$$R\left(t\right) = 2.04 * 0.43 I_P * 0.44\ T_{on} \tag{2}$$

This assumption is important to determine the radius of the discharge channel (spark) for each input current intensity case. The total heat flux generated and absorbed by the work piece, electrode and dielectric can be calculated assuming that the machining area is about 500 mm^2 and the effective geometric machining area is about 0.75% of the total machining area and about 10% of the total numbers of discharge sparks generated instantaneously during one pulse on period of time, then:

The total number of discharge sparks (*SN*) = Total machining area x 20% x 0.75 / Area of one discharge spark. (3)

The total heat fluxes entering the work piece, the electrode and the dielectric fluid during the on-time for all EDM experiments were calculated using Eq.(1), but this equation needs to be modified as:

$$Qw\,(r) = \frac{4.57 * Rw\ * Vb * Ip * Kn}{\pi . R^2} e^{-4.5\frac{r^2}{R^2}}\ \text{X SN / Machining area of the work piece} \tag{4}$$

Eq. (4) can be calculated for each EDM parameter taking into account all the above factors of modifications and for ($r = R$) at the end of pulse on duration time, and then the results for the total heat fluxes entering the work piece, the electrode and the dielectric fluid during the on-time for all PMEDM experiments are given in Table 5. The theoretical and numerical total heat flux generated by the using copper and graphite electrodes and FEM and ANSYS solutions for experimental group (2) is given in Table 6. The percentage increase in the value of the experimental total heat flux using SiC mixed powder (group 2) compared with (group 1) using kerosene dielectric alone are given in Table 7.

Table 4
The average values of material removal rate (MRR) and the experimentally estimated values of (Kn) factor for all EDM and PMEDM machining groups.

Exp. No.	Type of electrode	Pulse on time T_{on} (μs)	Pulse off time T_{off} (μs)	Pulse current (A)	Material removal rate-average values (MRR) mm^3/min		Average values of *Kn* coefficient	
					Group 1 Av.	Group 2 Av.	Group 1	Group 2
1.	Copper	120	40	8	8.6789	12.7007	1.00	3.53
2.	Copper	120	40	22	27.2888	56.3795	1.00	4.74
3.	Copper	40	14	8	7.6445	8.7665	1.00	2.98
4.	Copper	40	14	22	16.4341	29.9636	1.00	4.37
5.	Graphite	120	40	8	7.0185	8.9378	0.75	3.07
6.	Graphite	120	40	22	34.4913	77.0086	1.40	4.84
7.	Graphite	40	14	8	9.7517	8.0047	1.24	2.21
8.	Graphite	40	14	22	24.7480	34.3113	1.82	2.77

© 2018 IAU, Arak Branch

Table 5
The total heat flux fraction values absorbed by the workpieces, the electrodes and kerosene dielectric for group (2).

Exp. No.	Type of electrode	Pulse on duration T_{on} (μs)	Pulse off duration T_{off} (μs)	Pulse current (A)	Heat flux percentage fraction absorbed by the : [MW/m^2]		
					Work piece	Electrode	Kerosene dielectric
1.	Copper	120	40	8	110.03	237.57	1004.57
2.	Copper	120	40	22	170.22	383.00	1554.11
3.	Copper	40	14	8	245.17	551.63	2238.40
4.	Copper	40	14	22	411.94	926.865	3761.01
5.	Graphite	120	40	8	71.77	161.48	655.26
6.	Graphite	120	40	22	300.53	676.19	2743.84
7.	Graphite	40	14	8	225.47	507.31	2058.54
8.	Graphite	40	14	22	475.24	1069.29	4338.94

Table 6
The experimental and numerical total heat flux (power) generated by PMEDM processes using kerosene dielectric with graphite mixed powder.

Exp. No.	Type of electrode	Pulse on time T_{on} (μs)	Pulse off time T_{off} (μs)	Pulse current (A)	Experimental total heat flux [MW/m^2]	Numerical total heat flux [MW/m^2]	Error in numerical mode %
1.	Copper	120	40	8	1325.17	1367.20	+3.2
2.	Copper	120	40	22	2107.33	2192.20	+4.0
3.	Copper	40	14	8	3035.20	3160.40	+4.1
4.	Copper	40	14	22	5099.81	5314.90	+4.2
5.	Graphite	120	40	8	888.51	822.75	-7.4
6.	Graphite	120	40	22	3720.56	3374.10	-9.3
7.	Graphite	40	14	8	2791.32	2537.00	-9.1
8.	Graphite	40	14	22	5883.47	5322.70	-9.5

Table 7
The experimental heat flux (power) generated by EDM (group 1) and PMEDM (group 2) processes.

Exp. No.	Type of electrode	Pulse on time T_{on} (μs)	Pulse off time T_{off} (μs)	Pulse current (A)	Experimental total heat flux [MW/m²]		Percentage increase in total heat flux (%)
					Group (1)	Group (2)	
1.	Copper	120	40	8	434.62	1325.17	+204.9
2.	Copper	120	40	22	531.88	2107.33	+296.2
3.	Copper	40	14	8	1218.50	3035.20	+149.1
4.	Copper	40	14	22	1396.12	5099.81	+265.3
5.	Graphite	120	40	8	346.26	888.51	+156.6
6.	Graphite	120	40	22	919.62	3720.56	+304.6
7.	Graphite	40	14	8	1511.00	2791.32	+84.7
8.	Graphite	40	14	22	2541.00	5883.47	+131.5

The maximum total heat flux generated by the discharge processes and obtained by the FEM and ANSYS solutions and simulations after EDM machining using the copper and graphite electrodes for group (2) are given in Fig. 4. This figure shows two simulations models for maximum values of input EDM parameters using copper and graphite electrodes, respectively. The right figures represent the total heat flux generated form of the electrode, the work piece and the kerosene dielectric. The figures in the left show the thermal model of the electrode and work piece with the values of maximum heat flux generated and the input EDM and PMEDM processes parameters and also the verified percentage errors between the experimental thermal models compared with the theoretical calculations.

Three levels factorial response surface methodology (RSM) and the design expert 9.0 software were used to analyze the obtained total heat flux for each parametric subgroup, the analysis results for both experimental groups using the copper and graphite electrodes are shown in Fig. 5 and 6.

© 2018 IAU, Arak Branch

The predicted equation of the total heat flux generated for PMEDM experimental group (2), using copper electrodes and kerosene dielectric with graphite powder mixing, is:

$$\text{Total heat power} = +2741.80196+156.15304 * \text{Pulse current}-27.31834 * \text{Pulse on time } (T_{on}) \quad (5)$$

And, using graphite electrodes is:

$$\text{Total heat power} =+3164.28946+156.15304*\text{Pulse current}-27.31834 * \text{Pulse on time } (T_{on}) \quad (6)$$

The total heat flux generated for experimental group (2), using the copper electrodes and graphite mixing powder, the total heat flux values reached the maximum value as (5.315E +009 W/m^2). While, when using the graphite electrodes, the total heat flux values reached the maximum value as (5.323E+009 W/m^2) at the same input current and time on period.

This means that the use of graphite electrodes and the kerosene dielectric with graphite mixed powder yields the same total heat flux values when compared with the use of copper electrodes. These values give more heat flux generated when using the copper electrode and dielectric alone by (270.1 %) and more than when using the graphite electrodes and the kerosene dielectric alone by (102.9 %).

The high total heat flux levels are obtained when using the graphite or copper electrodes and the graphite mixed powder because of the abrasive graphite powder which works on enlarging the electrodes gaps and more arrangement of the discharge plasma channels.

Exp. No.	Type of electrode	Pulse on duration T_{on} (μs)	Pulse Current (A)
4.	Copper	40	22
Total heat flux = 5.315E+009 W/m^2 (+4.2%)			
8.	Graphite	40	22
Total heat flux = 5.323E+009 W/m^2 (-9.5%)			

The total heat flux
W/m^2

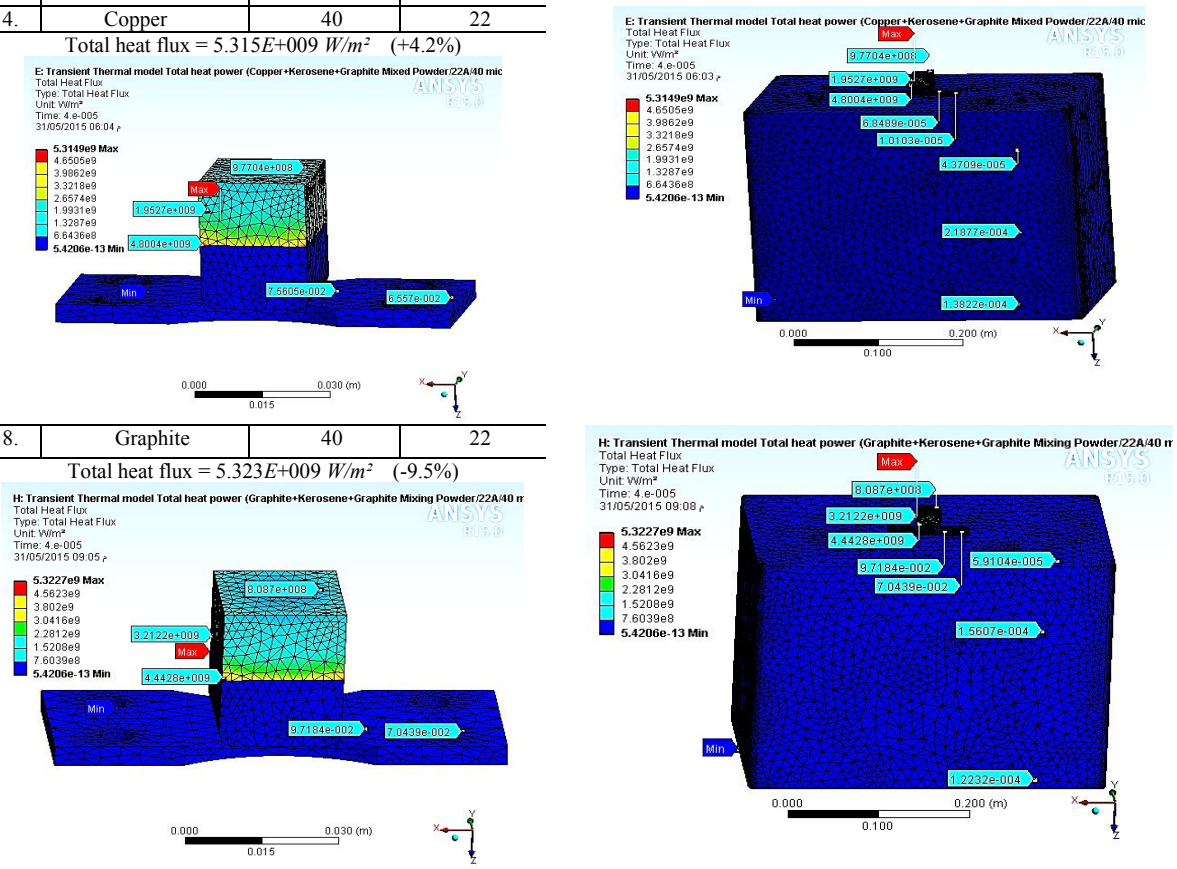

Fig. 4
The total modeled heat flux generated by the PMEDM experiments using the graphite powder, the pulse current (22 A) and the pulse on time (40 μs).

© 2018 IAU, Arak Branch

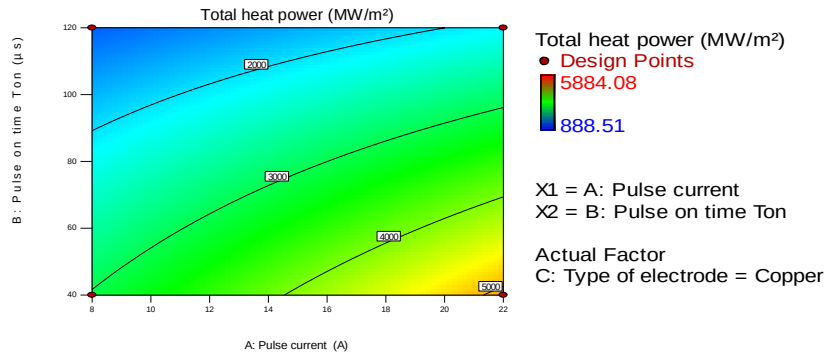

Group (2) / EDM + Kerosene dielectric + Graphite powder mixing

Fig.5
The total heat flux (power) generated by the EDM machining using copper electrodes and graphite powder mixing.

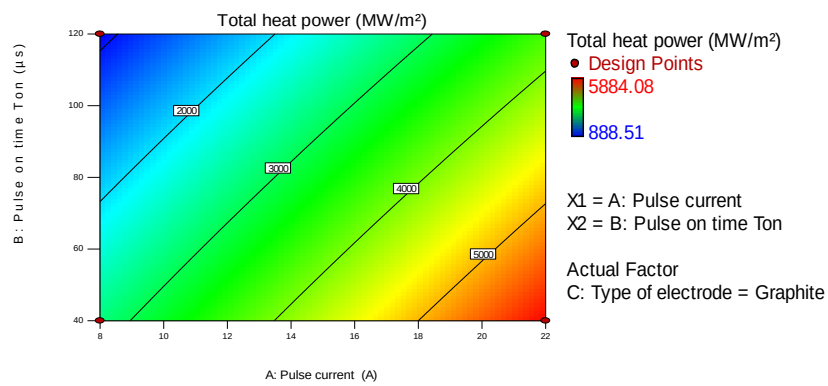

Group (2) / EDM + Kerosene dielectric +Graphite powder mixing.

Fig.6
The total heat flux (power) generated by the EDM using graphite electrodes and graphite powder mixing.

4 CALCULATION THE WHITE LAYER THICKNESS (WLT)

The average of three values of work pieces WLT measurements after EDM machining for both experiments using the two groups is given in Table 8. The predicted equation of WLT for EDM machining, using copper electrodes and graphite mixed powder obtained from the using three levels factorial response surface methodology (RSM) and the design expert 9.0 software, is:

$$\text{WLT} = +8.25589 - 0.18089 * \text{Pulse current} + 0.18441 * \text{Pulse on time } (T_{on}) \quad (7)$$

And, for graphite electrodes is:

$$\text{WLT} = +12.42339 - 0.18089 * \text{Pulse current} + 0.18441 * \text{Pulse on time } (T_{on}) \quad (8)$$

The average of WLT for after PMEDM machining using the copper and graphite electrodes is shown in Fig. 7 and 8, respectively. For experimental groups (2) using the graphite mixed powder and copper electrodes, the WLT reached the minimum value as (10.0 μm) at a current value of (22 A) and a pulse time of (40 μs), while when using the graphite electrodes, the WLT reached the minimum values as (16.67μm) at the input current (8 A) and with the same time on period (40 μs), as shown in Fig. 7. This means that an improvement by (66.7 %) was obtained when using copper electrodes compared with using graphite electrodes.

© 2018 IAU, Arak Branch

The lower levels of the obtained WLT when using the copper electrodes and the abrasive graphite work on removal of the melted white layer at moderate rates by micro shot peening process in a short period of time together with a high spark discharge heat power produced due to the good arrangements of the plasma discharge channels that enlarge the gap between the electrodes by about three times which works on increasing the discharge power too, with the use of dielectric flushing from both sides of the cutting zone.

The figures in Table 9, show the macro graphic and microstructure of the heat affected zones (HAZ) for the work pieces surfaces for each subgroups input parameters after PMEDM processes using copper and graphite electrodes. These figures show that the craters sizes increased with increasing the pulse current and the time on duration and they reached their minimum sizes, especially when using the graphite electrodes, where higher plasma discharge heat power was generated. The construction of these microscopic layers and HAZ for experimental group (2) indicates that lower layer thicknesses and defects exist due to the moderate abrasive and micro shot peening properties of the graphite powder and the plasma discharge pressure of the process as well as the high role of the dielectric flushing of the formed craters from both sides of the cutting areas. With high pulse current value and time on duration, the defect sizes increase in these layers, especially when using the copper electrodes due to the high thermal energy generated.

Table 8
Calculation the average values of the white layer thickness (WLT) after EDM and PMEDM machining.

Exp. No.	Type of electrode	Pulse on T_{on} (μs)	Pulse off T_{off} (μs)	Pulse current (A)	Average WLT Group (1) (μm)	Average WLT Group (2)(μm)
1.	Copper	120	40	8	33.34	31.17
2.	Copper	120	40	22	26.67	24.44
3.	Copper	40	14	8	13.34	15.57
4.	Copper	40	14	22	11.67	10.00
5.	Graphite	120	40	8	20.00	31.17
6.	Graphite	120	40	22	8.34	32.24
7.	Graphite	40	14	8	15.00	16.67
8.	Graphite	40	14	22	15.00	17.77

Table 9
The WLT and HAZ microstructures for PMEDM group (2) using kerosene dielectric and graphite mixed powder.

Exp. No.	Type of electrode	Pulse on duration T_{on} (μs)	Pulse Current (A)	The white layer microstructure (optical microscope X300)
1.	Copper	120	8	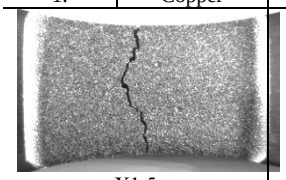 X1.5 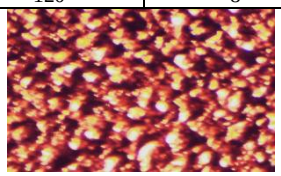 X40 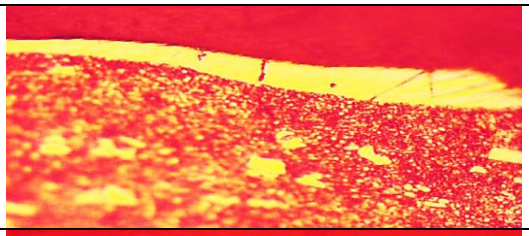
2.	Copper	120	22	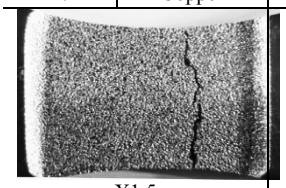 X1.5 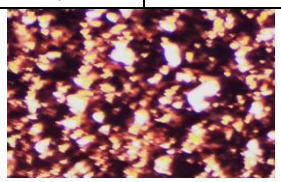 X40
3.	Copper	40	8	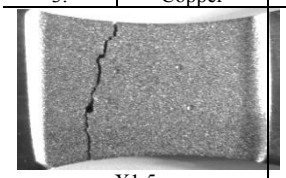 X1.5 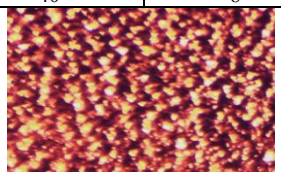 X40 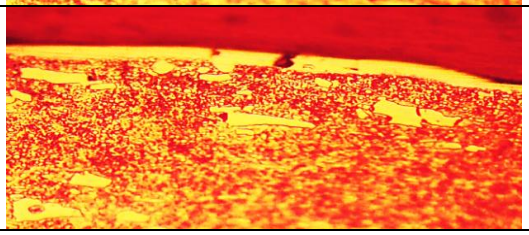

© 2018 IAU, Arak Branch

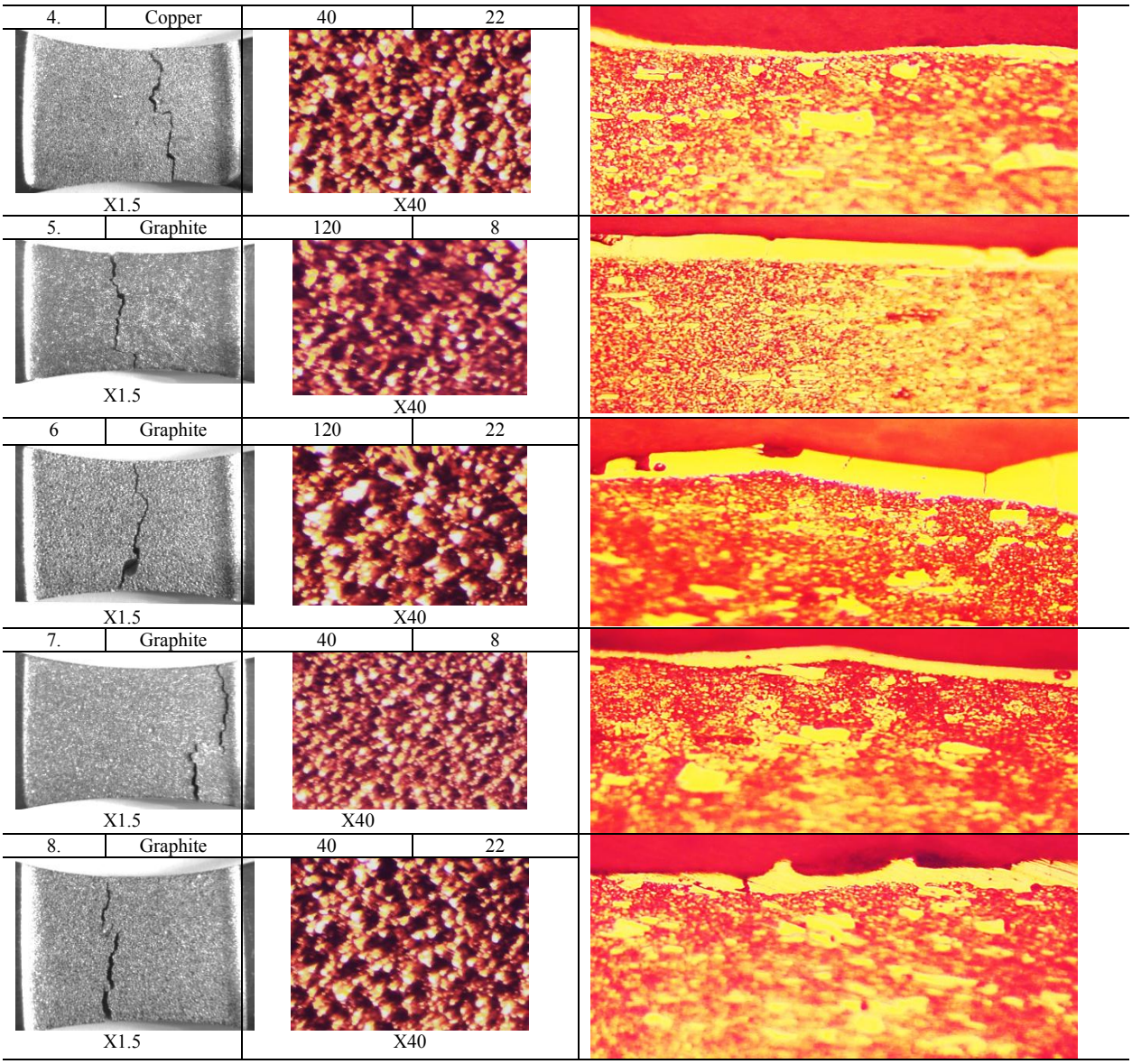

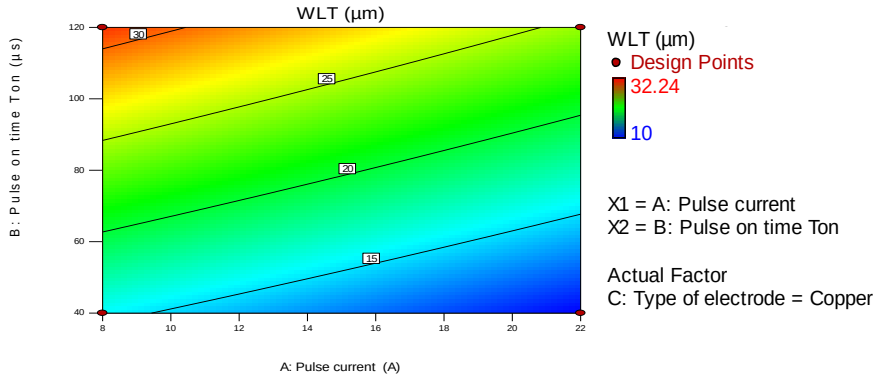

Group (2) / EDM + Kerosene dielectric +Graphite powder mixing.

Fig.7
The WLT for experimental group (2) after PMEDM using copper electrodes.

© 2018 IAU, Arak Branch

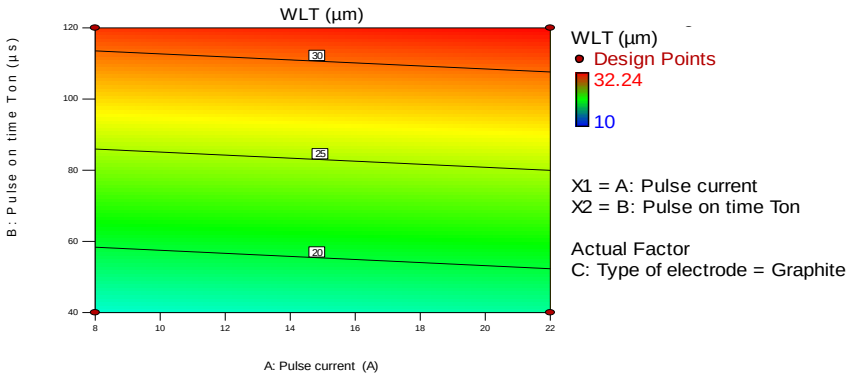

Group (2) / EDM + Kerosene dielectric +Graphite powder mixing.

Fig.8
The WLT for experimental group (2) after PMEDM using graphite electrodes.

5 MODELING AND SIMULATION THE FATIGUE LIFE USING FEM

In the present work, the high-cycle fatigue three-dimensional analysis and modeling for EDM of AISI D2 die steel was studied. The damage model was developed to study the influence of different parameters on the work piece fatigue life. This study used the stress life fatigue modeling analysis by using the ANSYS software 15.0. The cyclic fatigue of a material was obtained from completely reversed, constant amplitude tests with a load ratio of (-1) at room temperature. The Goodman mean stress correction theory is a good choice for brittle materials. The flat bending work pieces were used for the fatigue test. The test frequency of the machine was maintained constant at 60 *Hz*. The entire fatigue limit was defined at the stress level of (106) loading cycles. The Von-Mises stress theory which takes the sign of the largest absolute principal stress will be used to compare against the experimental stress value.

The Multiphysics, static structural models domain loads, include the environment temperature, the fixing supported and the loading force. The fatigue strength concentration factor (K_f), which is equal to (1) and (0.72) for flat as received specimens and for PMEDM machining work pieces [14], respectively was set. The experimental fatigue results after EDM and PMEDM machining are given in Table 10.

The experimental average values of fatigue stress at (10^6 cycles) and the experimental and numerical fatigue safety factor values for group (2) are given in Table 11., where the fatigue safety factor values were calculated as the ratio of fatigue stress at (10^6 cycles) of the experimental result respect to the fatigue stress at (10^6 cycles) of the as-received material which is equal to (270 *MPa*). The percentage enhancement in the value of experimental fatigue stresses at (10^6 cycles) using SiC mixed powder (group 2) compared with (group 1) using kerosene dielectric alone are given in Table 12.

The maximum fatigue life and safety factor obtained by the FEM and PMEDM with ANSYS solutions and simulations using the copper and graphite electrodes using the pulse current (8 *A*) and pulse on time (120 μs) are given in Fig. 9. Each simulation model in this figure shows two models for each of input parameters of PMEDM sub-group. The right figures represent the numerical modeled fatigue safety factor. The figures in the left shows the fatigue life models simulations with the values of fatigue stresses at (10^6 cycles) obtained from the *S/N* curves of each experimental sub-group, the input EDM process parameters and the model loading force.

The *S/N* fatigue stress at (10^6 cycles) curves for both groups after EDM and PMEDM machining, are shown in Fig. 10 and 11 using pulse current (8 *A*) and (22 *A*), respectively. These figures show that, fatigue life increasing with decreasing the pulse current and increasing the pulse on duration time, and copper electrodes gave fatigue life values higher than graphite electrodes, after EDM experimental group (1). Whereas, copper electrodes gave fatigue life values higher than graphite electrodes after PMEDM experimental group (2) and fatigue life increases with the decrease in pulse current values and pulse on duration time. These figures shows that the use of copper electrodes with graphite powder mixing improved the fatigue life and it is not recommended to adding the graphite powder when using the graphite electrodes as it is produces the lowest fatigue lives.

© 2018 IAU, Arak Branch

Table 10
The experimental fatigue life results for group (1) after EDM machining.

Exp. No.	Type of electrode	Pulse on time T_{on} (μs)	Pulse current (A)	Pulse off time T_{off} (μs)	For group (1)		For group (2)	
					Applied stress (σ) (MPa)	No. of cycles to failure (X1000)	Applied stress (σ) (MPa)	No. of cycles to failure (X1000)
1.	Copper	120	8	40	350.00	100.250	350.00	123.250
2.	Copper	120	8	40	300.00	239.750	300.00	271.500
3.	Copper	120	8	40	230.00	1260.500	250.00	1051.750
4.	Copper	120	22	40	350.00	61.000	350.00	133.000
5.	Copper	120	22	40	300.00	133.500	300.00	341.750
6.	Copper	120	22	40	215.00	1273.250	250.00	1215.250
7.	Copper	40	8	14	350.00	84.250	350.00	188.500
8.	Copper	40	8	14	300.00	199.750	300.00	481.000
9.	Copper	40	8	14	220.00	1157.500	270.00	1371.000
10.	Copper	40	22	14	350.00	56.250	350.00	94.750
11.	Copper	40	22	14	210.00	1212.500	240.00	1176.250
12.	Graphite	120	8	40	350.00	94.500	350.00	63.500
13.	Graphite	120	8	40	300.00	214.750	300.00	134.250
14.	Graphite	120	8	40	220.00	1319.000	210.00	1268.000
15.	Graphite	120	22	4	350.00	45.250	350.00	41.000
16.	Graphite	120	22	40	300.00	87.250	300.00	81.000
17.	Graphite	120	22	40	200.00	1063.750	210.00	1113.750
18.	Graphite	40	8	14	350.00	70.250	350.00	51.750
19.	Graphite	40	8	14	300.00	164.750	200.00	1063.000
20.	Graphite	40	8	14	215.00	1201.500	-	-
21.	Graphite	40	22	14	350.00	51.250	350.00	34.750
22.	Graphite	40	22	14	200.00	1188.500	200.00	1054.000

Table 11
The experimental average values of fatigue stress at (10^6 cycles) and fatigue safety factor for group (2) PMEDM machining with graphite powder mixing.

Exp. No.	Type of electrode	Pulse on time T_{on} (μs)	Pulse off time T_{off} (μs)	Pulse current (A)	Fatigue stress at 106 Cycles (MPa)	Fatigue Safety factor experiment	Fatigue safety factor numeric	Error in numeric mode%
1.	Copper	120	40	8	254	0.94	0.96	+2.1
2.	Copper	120	40	22	257	0.95	0.98	+3.2
3.	Copper	40	14	8	278	1.03	1.13	+10.8
4.	Copper	40	14	22	247	0.92	0.90	-2.2
5.	Graphite	120	40	8	220	0.82	0.72	-12.2
6.	Graphite	120	40	22	214	0.79	0.75	-5.1
7.	Graphite	40	14	8	203	0.75	0.66	-12.0
8.	Graphite	40	14	22	202	0.75	0.65	-13.3

Table 12
The experimental values of fatigue stress at (10^6 cycles) for EDM group (1) and PMEDM group (2).

Exp. No.	Type of electrode	Pulse on time T_{on} (μs)	Pulse off time T_{off} (μs)	Pulse current (A)	Experimental fatigue stress at 106 Cycles (MPa)		Percentage enhancement in fatigue stress (%)
					Group (1)	Group (2)	
1.	Copper	120	40	8	240	254	+5.8
2.	Copper	120	40	22	225	257	+14.2
3.	Copper	40	14	8	227	278	+22.5
4.	Copper	40	14	22	215	247	+14.9
5.	Graphite	120	40	8	232	220	-5.2
6.	Graphite	120	40	22	203	214	+5.4
7.	Graphite	40	14	8	223	203	-9.0
8.	Graphite	40	14	22	207	202	-2.4

© 2018 IAU, Arak Branch

Exp. No.	Type of electrode	Pulse on duration Ton (μs)	Pulse Current (A)	Fatigue Safety Factor
3.	Copper	40	8	Fatigue Safety Factor = 1.13
Fatigue life=1.37E+6Cycles / σb=278MPa / F=147N				
5.	Graphite	120	8	Fatigue Safety Factor=0.72
Fatigue life=1.27E+6Cycles / σb=220MPa / F=179N				

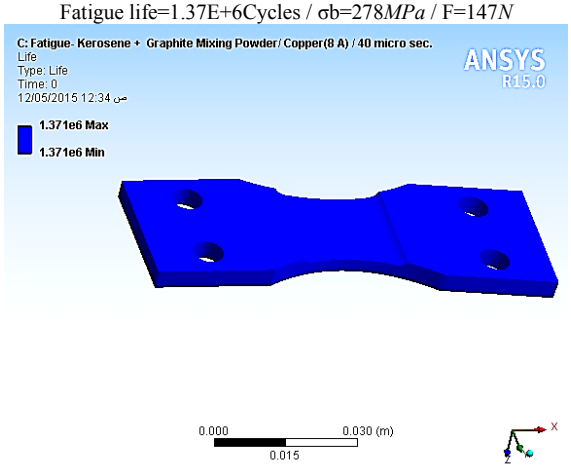

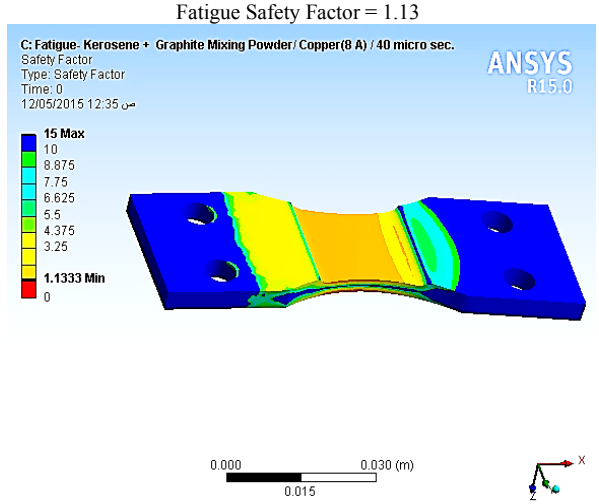

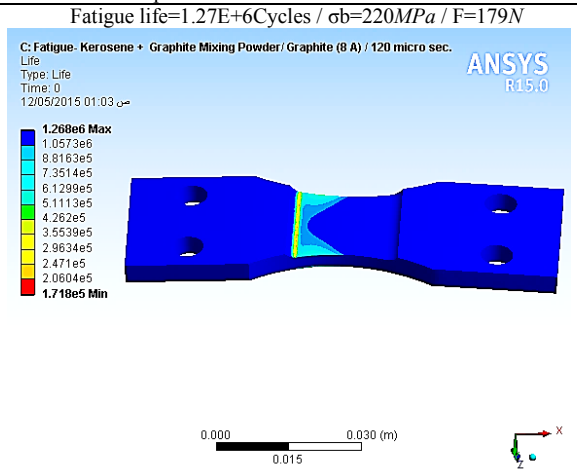

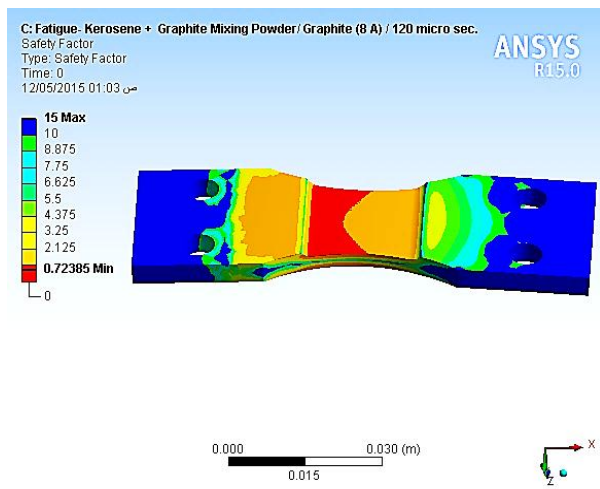

Fig. 9
The FEM fatigue life and safety factor Models for PMEDM machining of group (2) with graphite powder mixing.

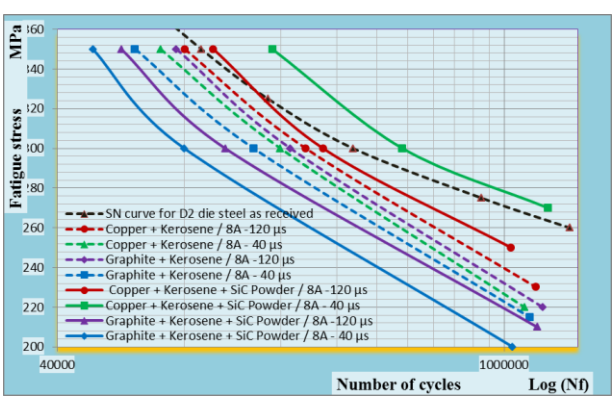

Fig. 10
The *S/N* curves of experimental groups (1) and (2) after EDM and PMEDM using the graphite powder mixing and pulse current (8 *A*).

© 2018 IAU, Arak Branch

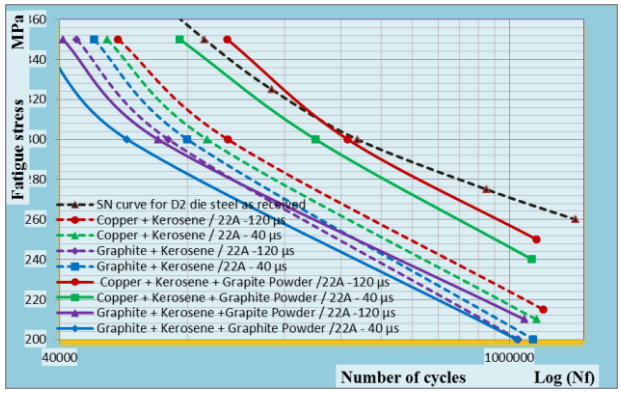

Fig. 11
The S/N curves for experimental groups (1) and (2) after EDM and PMEDM using the graphite powder mixing and pulse current (22 *A*).

The three levels factorial response surface methodology (RSM) and the design expert 9.0 software were used to analyze the obtained fatigue safety factor for each parametric subgroup.

The predicted equation of the fatigue safety factor for PMEDM experimental group (2), using kerosene dielectric with graphite mixing powder and copper electrodes, is:

Fatigue Safety Factor=+1.02589-3.39286E-003*Pulse current+ 2.18750E -004* Pulse on time (T_{on}) (9)

And, using graphite electrodes is:

Fatigue Safety Factor=+0.72839-3.39286E-003*Pulse current+2.18750E -004* Pulse on time (T_{on}) (10)

The predicted equation of the fatigue stress at (106 cycles) obtained by using copper electrodes is:

Fatigue stress at 106 cycles = +264.62500-0.62500 * Pulse current time +0.046875* Pulse on time (T_{on}) (11)

And, using graphite electrodes is:

Fatigue stress at 106 cycles = +215.37500-0.62500* Pulse current time +0.046875* Pulse on time (T_{on}) (12)

The results of analysis for fatigue safety factor for all experiments using the copper and graphite electrodes are shown in Fig. 12 and 13, respectively. While, the fatigue stresses at (106 cycles) for all experimental groups using the copper and graphite electrodes are shown in Fig. 14 and 15, respectively. The fatigue safety factor using the copper electrodes for experimental group (2) increases with the decrease in pulse current values and pulse on duration time, reaching the maximum value as (1.13), experimentally (1.03) at a current value of (8 *A*), a pulse time of (40 μs). While, when using the graphite electrodes, the fatigue safety factor values reached their maximum value as (0.75), experimentally (0.79) at high input current (22 *A*) and pulse on time period (120 μs), as shown in Fig. 13. This means that the use of copper electrodes and the kerosene dielectric with graphite mixed powder gives higher experimental fatigue safety factor values by (30.38 %) when compared with the using of graphite electrodes and higher by (15.73%) and (19.77%) when compared with the results of group (1) using the copper and graphite electrodes, respectively. The fatigue stresses at (10^6 cycles) after PMEDM experimental group (2) using the copper electrodes are increasing with the decrease in pulse current and the pulse on duration time, reaching the maximum value as (278 *MPa*) at a current value of (8 *A*), pulse on time (40 μs).

While, when using the graphite electrodes, these fatigue stress values reached the maximum value as (220 *MPa*) at the same input current and higher pulse on period time (120 μs), as shown in Fig. 14 and 15. This means that the use of copper electrodes and the kerosene dielectric with graphite powder mixing yields fatigue stresses at (10^6 cycles) values higher by (26.36 %) when compared with using graphite electrodes and gives a higher fatigue life than the situation when working without mixed powder by (15.83 %) and (19.83 %) using the copper and graphite electrodes, respectively.

© 2018 IAU, Arak Branch

The stress values are equal to the ratios (1.03) and (0.77) for copper and graphite electrodes, respectively compared with the fatigue stresses at (10^6 cycles) for the as-received material. These stress values are very close to those of fatigue safety factors for the same input parameters of the process for this experimental group as well as all the other experimental groups, which have just discussed, and this proves the accuracy of all EDM and PMEDM models developed by ANSYS.

The abrasive characteristics of graphite powder , which are working on micro shot peening of the machining surfaces, produce a lower brittle carbides formation, fewer defects and lower white layer thickness, and all these factors strengthen the work piece against fatigue failure and then longer lives are obtained. While, the graphite electrodes with graphite powder mixing work on increasing the carbide formation by the migration of the carbon particles from the electrode to the work piece, and consequentially weak surfaces are obtained with lower values of fatigue safety factors.

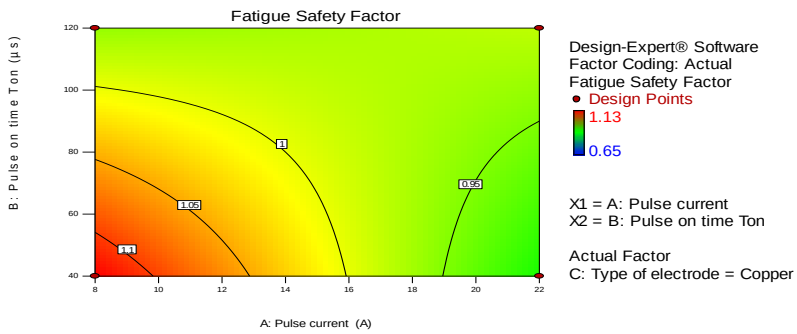

Fig. 12
The fatigue safety factor after PMEDM using copper electrodes and graphite mixed powder.

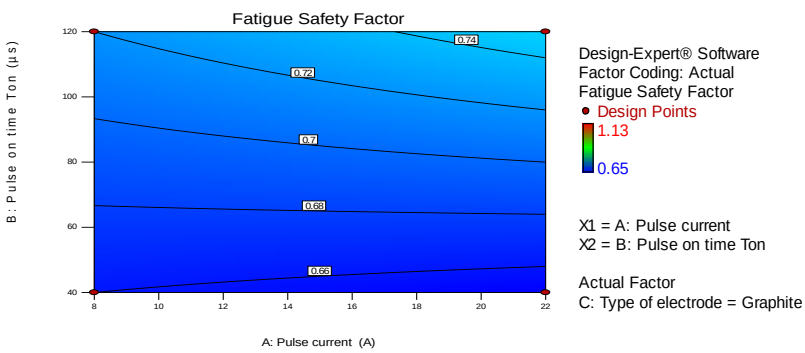

Fig. 13
The fatigue safety factor after PMEDM using graphite electrodes and graphite mixed powder.

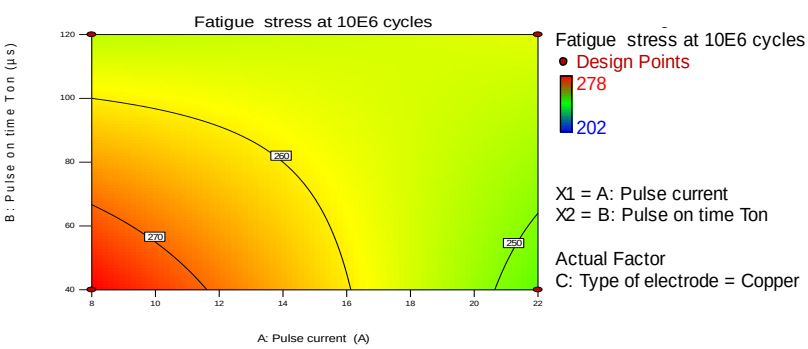

Fig. 14
The fatigue stresses at (106cycles) after PMEDM using copper electrodes and graphite mixed powder.

© 2018 IAU, Arak Branch

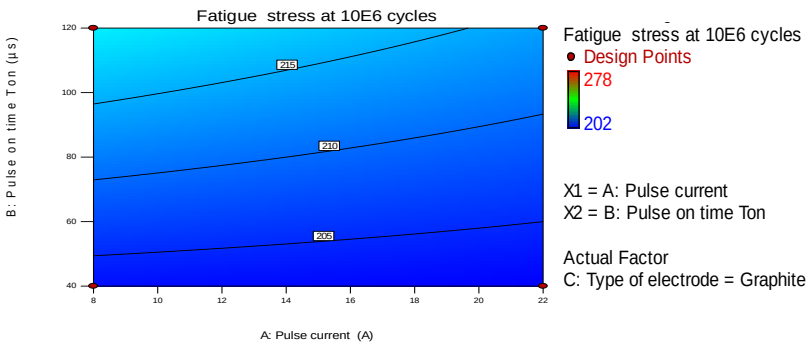

Fig. 15
The fatigue stresses at (106cycles) after PMEDM using graphite electrodes and graphite mixed powder.

6 CONCLUSIONS

1. The total heat power values are increasing with the increase of pulse current values up to (22 *A*) and the decrease of pulse on duration time to (40 μs).
2. The use of graphite powder and both electrodes gave more heat power by (270.1 %) and (102.9 %) than the copper and graphite electrodes, respectively with using the kerosene dielectric alone.
3. The WLT reached its minimum value of (8.34 μm) using the kerosene dielectric alone and graphite electrodes at higher values of pulse current and pulse on time. This means an improvement by (40.0 %) when compared with the use of copper electrodes.
4. The WLT reached its minimum value of (10.0 μm) at high current and low pulse on time using the copper electrodes and the graphite powder. This means that an improvement by (66.7 %) was obtained when compared with the use of graphite electrodes under the same machining conditions.
5. Copper electrodes with graphite powder yielded experimental fatigue safety factor values of (1.03), which is higher by (30.38 %) when compared with using graphite electrodes and higher by (15.73%) and (19.77%) when compared with results of group (1) using the kerosene dielectric alone and copper and graphite electrodes, respectively.
6. Copper with graphite powder gives fatigue stresses of (278 *MPa*), which is higher by (26.36 %) when compared with the use of graphite electrodes and yielded a higher fatigue life than the situation when working without mixing powder by (15.83 %) and (19.83 %) using the copper and graphite electrodes, respectively.

REFERENCES

[1] Lee L.C., Lim L.C., Wong Y.S., Lu H.H., 1990, Towards a better understanding of the surface features of electro-discharge machined tool steels, *The Journal of Materials Processing Technology* **24**: 513-523.

[2] Lim L.C., Lee L.C., Wong Y.S., Lu H.H. 1991, Solidification microstructure of electro discharge machined surfaces of tool steels, *Journal of Materials Science and Technology* **7**: 239-248.

[3] Lin Y.C., Yan B.H., Huang F.Y., 2001, Surface improvement using a combination of electrical discharge machining with ball burnish machining based on the Taguchi method, *The International Journal of Advanced Manufacturing Technology* **18**(9): 673-682.

[4] Abu Zeid O.A., Ho K.H., Newman S.T., 2003, On the effect of electro-discharge machining, *International Journal of Machine Tools & Manufacture* **43**: 1287-1300.

[5] Khundrakpam N.S., Singh H., Kumar S., Brar G.S., 2014, Investigation and modeling of silicon powder mixed EDM using response surface method, *International Journal of Current Engineering and Technology* **4**(2): 1022-1026.

[6] Reddy B., Kumar G.N., Chandrashekar K., 2014, Experimental investigation on process performance of powder mixed electric discharge machining of AISI D3 steel and EN-31 steel, *International Journal of Current Engineering and Technology* **4**(3): 1218-1222.

[7] ASTM A370, Standard Test Method and Definitions for Mechanical Testing of Steel Products, American Society for Testing and Materials, Washington.

[8] ASTM A681, Standard Specification for Tool Steels Alloy, American Society for Testing and Materials, Washington.

© 2018 IAU, Arak Branch

[9] Bhattacharya R., Jain V.K., Ghoshdastidar P.S., 1996, Numerical simulation of thermal erosion in EDM process, *Journal of the Institution of Engineers Part PR, Production Engineering Division* **77**: 13-19.
[10] Yadav V., Jain V.K., Dixit P.M., 2002, Thermal stresses due to electrical discharge machining, *International Journal of Machine Tools and Manufacture* **42**: 877-888.
[11] Patel B.B., Rathod K.B., 2012, Multi-parameter analysis and modeling of surface roughness in electro cischarge machining of AISI D2 steel, *International Journal of Scientific & Engineering Research* **3**(6): 1-6.
[12] Shankar P., Jain V.K., Sundarajan T., 1997, Analysis of spark profiles during EDM process, *Machining Science Technolog*y **1**(2): 195-217.
[13] Marafona J., Chousal J.A., 2006, A finite element model of EDM based on the Joule effect, *International Journal of Machine Tools and Manufacture* **46**: 595-602.
[14] Shigley J.E., Mischke C.R., 2006, *Mechanical Engineering Design*, McGraw-Hill Inc.

© 2018 IAU, Arak Branch